DOI: 10.31577/ahs-2026-0027.01.0016

ACTA HYDROLOGICA SLOVACA

Volume 27, No. 1, 2026, 149 – 159

Suspended sediment load and discharge relationships: Insights from long-term monitoring in the Bedog River, Indonesia

Aqila Rheva Latifah IBRAHIM, Lintang Nur FADLILLAH*

This study aims to analyze the correlations between water level and river discharge, as well as between discharge and suspended sediment. Estimates of the total suspended sediment load in Bedog Watershed, Yogyakarta, Indonesia are provided as well. The Bedog Sub-watershed, located on the southern slope of Mount Merapi wasonly slightly affected by the 2010 eruption. Data were obtained through continuous water level monitoring and depth-integrated suspended sediment sampling, with field observations conducted during the rainy season (November 2024–April 2025). Statistical analysis was conducted using Pearson correlation. Strong positive correlations were identified during both the rising (r=0.95) and falling (r=0.99) phases of the hydrograph, as well as between discharge and suspended sediment during the ascending (r=0.97) and descending (r=0.93) phases. Estimated annual suspended sediment load from 2015 to 2024 ranged from 3,360.59 to 4,550.29 tons year^{-1}, with sediment yield classified as very low, ranging from 0.291 to 0.393 tons ha^{-1} year^{-1}.

KEY WORDS: hydrograph, landuse change, river sediment, sediment yield, total suspended sediments (TSS)

Introduction

Rivers are key components of watersheds, which are natural ecosystems defined by topographic boundaries and surrounding ridges. Rivers serve as sediment transport channels. This function can lead to siltation, reducing their capacity to convey water efficiently and increasing flood risk (Mahmood et al., 2022). Siltation results from erosion and sedimentation, which are influenced by flow velocity. Fast upstream flows cause strong erosion and transport materials downstream, while gentler slopes in the middle reaches reduce erosion, and slower currents downstream promote sediment deposition. Continuous upstream erosion supplies soil that is carried and deposited downstream, shaping sedimentation patterns throughout the watershed.

The Bedog River originates on the southern slope of Mount Merapi, unaffected by the 2010 eruption, and flows into the Progo River (Suprayogi et al., 2019). It is a perennial river supported by high rainfall and permeable soils with thick aquifers. Unlike rivers directly impacted by the eruption, studying sediment in the Bedog Sub-watershed offers novelty and valuable input for watershed management. According to data from the Department of Environment and Forestry of Yogyakarta Province (2025), the downstream Bedog River recorded the third highest Total Suspended Sediment (TSS) in 2024, after the Winongo and Konteng Rivers. This condition is important to study because TSS is often used to assess watershed health, whether it is in good condition, requires maintenance, or is degraded and needs restoration (Setiawan et al., 2025) (Fig.1).

Measuring sediment transport is complex because it is influenced by particle size, density, and river flow dynamics (Soewarno, 1991). Suspended sediment concentration is commonly used as an indicator of sediment transport and related processes, reflecting water dynamics and quality (Shenliang et al., 2003; Vercruysse et al., 2017). This study assumes that all transported sediment is deposited downstream for sampling and calculation. The ten-year suspension load is expected to provide a representative picture for watershed management, since high sediment levels indicate serious sedimentation issues requiring attention. The Bedog Sub-watershed, which faces settlement-driven land conversion, is therefore a management priority and plays an important role in supporting ecosystems and communities within Yogyakarta's hydrological system. According Hermawan et al. (2025), effective management can be supported through monitoring water level, discharge, and suspended sediment.

Material and methods

Research Location

The research site covers the 115.6 km² Bedog Sub-watershed, located on the southern slope of Mount

Merapi and forming part of the downstream Progo watershed in Sleman Regency (Suprayogi et al., 2019) (Fig. 2). The sub-watershed faces land use change from agriculture to residential and industrial areas, leading to ecological degradation and reduced environmental carrying capacity (Adhitama et al., 2022). The Bedog River cross section is overgrown with water hyacinth plants. Water hyacinth is an aquatic plant that reproduces very quickly and is generally considered a weed. During the dry season, the volume of river water decreases so that the flowing current has a slower speed than during the rainy season. Water hyacinth survives by floating and not being carried away by the river current. In the rainy season, the presence of water hyacinth is no longer found because the collection of water hyacinth is carried away by the river current along with the increase in flow speed. From 2019 to 2024, land cover in the Bedog Sub-watershed has undergone significant changes, particularly the conversion of vegetated land into non-vegetated land (Table1). The area of vegetated land decreased from 59.6 km² in 2019 to 38 km² in 2024, whereas the non-vegetated land area increased from 56 km² in 2019 to 77.6 km² in 2024. As shown in Fig. 3, the central part of the watershed experienced a drastic

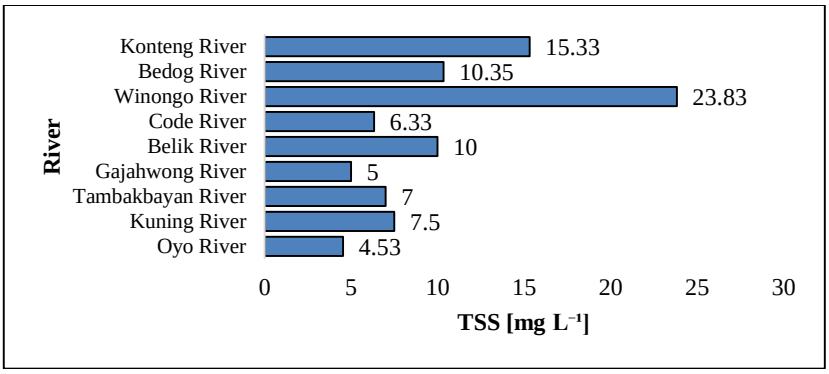


Fig. 1. Total Suspended Sediments (TSS) Load in the Downstream Segments of Rivers Crossing the Special Region of Yogyakarta in 2024.

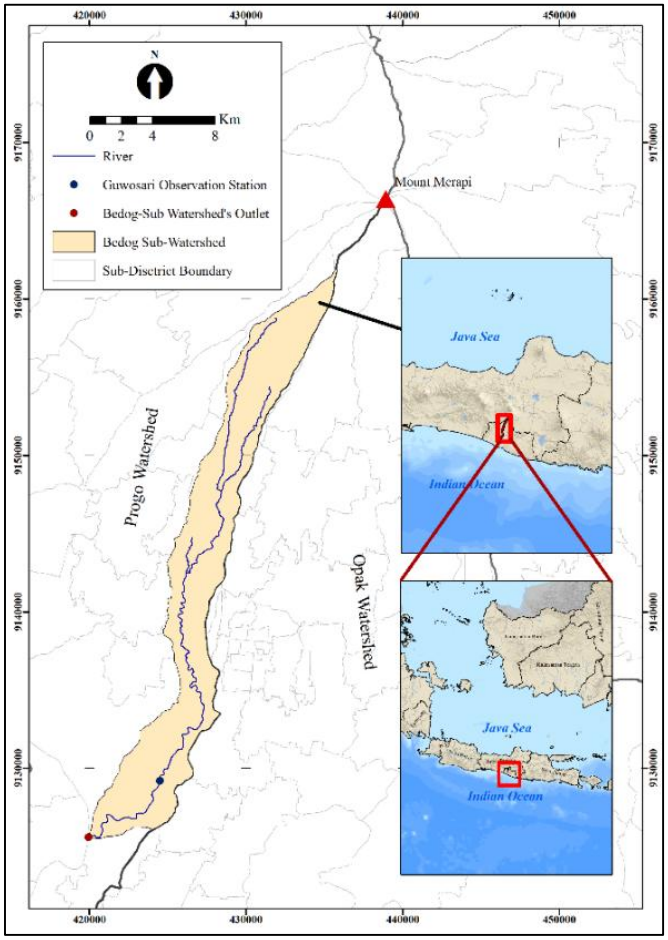


Fig. 2. Boundary Map of Bedog Sub-Watershed and Its Surroundings.

Table 1. Major Land Use Changes in Bedog Sub-Watershed (2019 and 2024) [km²]

Landcover	Year	
	2019	2024
Vegetation	59.6	38.0
Non-vegetation	56.0	77.6
Total	115.6	115.6

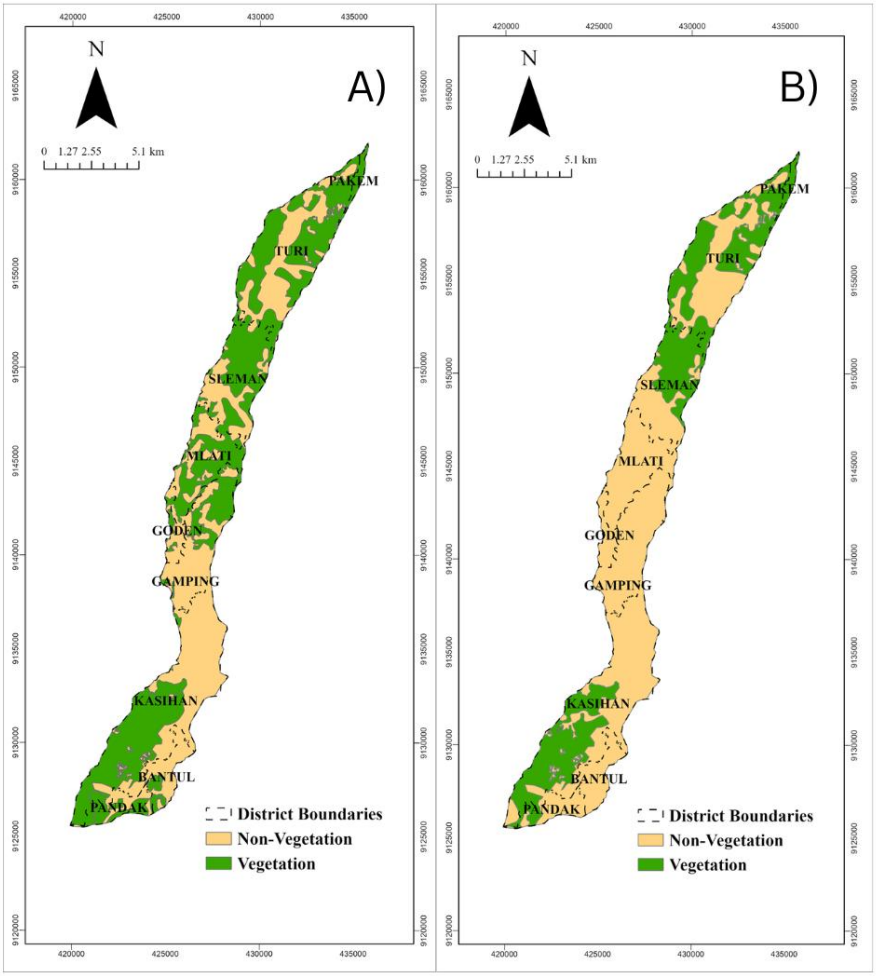


Fig. 3. Spatial variation in land cover within the Bedog Sub-Watershed from 2019 (a) to 2024 (b), indicating a decline in vegetated areas and an increase in non-vegetated land.

change in land use. Urbanization, particularly in Mlati District of Sleman Regency, has driven residential expansion. To address land degradation, conservation efforts such as tree planting are needed to maintain soil cover. According to Astuti and Lukito (2020), land conversion in Sleman Regency is driven by its appeal as an educational, residential, and tourism hub, along with declining rice field productivity that encourages owners to seek higher economic returns. Asrul et al. (2025) note that reduced vegetation cover alters water flow and decreases soil productivity. Nuraida et al. (2024) emphasize that such conditions increase erosion and sediment transport from upstream to downstream.

Collecting Samples

Water level observations were conducted using a water board (peilschaal) installed at the nearest outlet station. The peilschaal is a graduated vertical scale fixed to a stable structure in the river, which measures water level by direct visual reading of the water surface against the scale in meters. Measurements were recorded simultaneously with suspension sampling and were carried out at regular intervals, with additional observations taken after events that caused significant changes in water level, such as rainfall.

Microsoft Excel software was used to perform all

calculations and develop graphs.
River discharge (Q) was estimated at the same intervals and following significant changes in water level. The estimation was based on a rating curve developed at Serayu-Opak Basin Center for the Guwosari Station as shown in equation (1):

$$Q = 14.719\ (Water\ level - 0.571)^{2.205} \quad (1)$$

where
Q – is river discharge [m³ s⁻¹],
H – is the water level elevation [m], defined as the vertical distance of the water surface relative to the local gauge datum at the Guwosari Station.

Direct discharge measurements were not conducted simultaneously with suspension sampling, as the sampling process was performed rapidly and followed short-term fluctuations in water level, making it impractical to measure discharge directly using field instruments.
Suspended sediment sampling was conducted using a depth-integration technique at two vertical points across each cross-section. This method is effective during high-flow conditions when discharge and sediment cannot be measured simultaneously (Hicks and Fenwick, 1994). The sampling was performed by moving the sampler vertically at a constant speed from the water surface to near the riverbed to obtain depth-integrated samples representing suspended sediment concentration (Soewarno, 1991).
Sampling was carried out at two cross-sections (CS1 and CS2) within the study reach near Sindon Bridge, with a distance of approximately 9.4 m between them. At each cross-section, the effective flow width (W) was approximately 18.8 m, measured from the left to the right riverbank, excluding non-flow areas near the banks and bridge structures. Two vertical sampling points were selected to represent the left and right portions of the channel. Sampling was conducted at regular intervals and during events that caused significant changes in water level, such as rainfall. Although only two verticals were used, the selected points were considered sufficient to represent general sediment conditions within the relatively uniform study reach.

Data Processing of Suspended Sediment Samples

Sediment concentration was calculated using the gravimetric method, which is based on the difference in filter weight before and after filtration and drying. Sediment samples were analyzed to determine suspended sediment concentration using equation (2) developed by the American Public Health Association (APHA, 2017):

$$C_s = \frac{g_2 - g_1}{V} \quad (2)$$

where
C_s – sediment concentration [mg L⁻¹],
g_1 – weight of empty filter paper [mg],
g_2 – weight of empty filter paper and sediment [mg],
V – volume of filtered water (l).

The known sediment concentration is subsequently used to estimate the suspended sediment load which is at a given time period expressed in equation (3). This estimation follows the instantaneous suspended sediment discharge approach developed by Soewarno (1991):

$$Q_{si} = k \times C_s \times Q \quad (3)$$

where
Q_{si} – suspension discharge/sediment load [ton day^{-1}],
k – 0.0864,
C_s – sediment concentration [mg L⁻¹],
Q – river discharge [m³ s⁻¹].

Calculation of Discharge Rating Curve

The stage–discharge rating curve was developed from concurrent measurements of water level and discharge collected over a certain period. The relationship between stage and discharge is commonly represented using a power function, as shown in equation (4) derived by Rantz et al. (1982).

$$Q = a \cdot (H)^b \quad (4)$$

where
Q – flow discharge [m³ s⁻¹],
H – water level [m],
a, b – constants.

The constants a and b in this equation are derived from the power regression analysis of observed water level and discharge data. In this context, constant a represents the hydraulic characteristics of the river channel, such as its shape and roughness, while constant b reflects the sensitivity of discharge changes relative to the water level as determined by the geometry of the riverbed.

Calculation of Suspended Sediment Discharge Based on Sediment Discharge Curve

The relationship between flow discharge and suspension discharge can be known through the sediment rating curve. The curve is used to estimate sediment transport at a flow discharge. The equation (5), developed by Dorneles et al. (2024) is used to determine the suspension discharge:

$$Q_s = a \cdot (Q)^b \quad (5)$$

where
Q_s – suspended sediment discharge [ton day⁻¹],
Q – flow discharge [m³ s⁻¹],
a, b – constants.

The values of a and b are obtained through regression analysis of field-sampled sediment concentration and measured flow discharge, representing the hydro-geomorphological characteristics of the watershed.

Constant a serves as an index of soil erodibility and sediment availability, while constant b represents the erosive power of the river and the efficiency of the flow in transporting sediment.
By utilizing these derived constants, the suspended sediment load calculations were performed on a daily basis over a 10-year period from 2015 to 2024. This extensive temporal resolution was utilized to capture long-term trends and seasonal patterns, providing a comprehensive data series for the temporal variation analysis

Pearson Product Moment Correlation Test

The Pearson Product–Moment correlation coefficient "r" measures the strength and direction of the linear relationship between variables without implying causality and assumes that the data are normally distributed (Bonacci et al., 2025). The coefficient is calculated using equation (6) by Walpole et al. (2012):

$$r = \frac{\Sigma[(X_i-\bar{X})\cdot(Y_i-\bar{Y})]}{\sqrt{[\Sigma(X_i-\bar{X})^2\cdot\Sigma(Y_i-\bar{Y})^2]}} \quad (6)$$

Spearman Correlation Test

Spearman's rank correlation coefficient "r_s" was used to evaluate the strength and direction of the monotonic relationship between variables. Unlike Pearson correlation, Spearman correlation is based on ranked data and does not require the assumption of normal data distribution. The coefficient is calculated using equation (7) by Mukaka (2012).

$$r_s = 1 - \frac{6\cdot\Sigma({d_i}^2)}{n(n^2-1)} \quad (7)$$

where
r_s – Spearman correlation coefficient,
d_i – the difference between paired data ranks,
n – the number of data pairs.

Calculation of Total Suspended Sediment Load

The total suspension load was calculated using the sediment rating curve and daily discharge data (2015–2024) from Guwosari Station. Results in ton day^{-1} were summed into monthly and annual loads, then divided by watershed area to obtain ton ha^{-1} year^{-1} based on the Indonesian Minister of Environment Regulation No. 61/2014 (Table 2).

Data Processing

All data processing was carried out using Microsoft Excel, including sediment concentration analysis based on the gravimetric method, development of discharge rating curves, calculation of suspended sediment discharge, calculation of total suspended sediment load, and statistical analyses (Pearson and Spearman correlation tests). Graphs, including hydrographs and rating curves, were also generated using the same software.

Results and discussion

Correlation Between Water Level and Discharge

Changes in river discharge are important to be understood as a fundamental basis for water resource management. The hydrographs presented are not merely to show the relationship between water level, discharge, and time, but also serve as a representation to understand the integrated response of the physiographic characteristics of the river basin to rainfall inputs over a temporal scale spanning several years. Hydrographs can also detect environmental changes, such as land use changes that cause non-stationary patterns in the hydrological system. The hydrograph showing the relationship between water level and discharge over time for the period 2015–2024 on the Bedog River is shown in Fig. 4.
Based on Fig. 4, it can be seen that the hydrograph shows several patterns, namely that the water level and flow rate will rise at the end of the year and the beginning of the year, which can be concluded that during the rainy season (October–April) there is an increase in the hydrograph. Meanwhile, the transition from the beginning of the year to the middle to the end of the year shows that the water level and flow rate decrease during the dry season, from April to October. This pattern shows that water levels and discharge are indirectly a direct response of the river basin system. However, this is also influenced by the physical characteristics of the Bedog Sub-watershed such as watershed shape, slope, and land use conditions. These hydrographs are important for flood analysis, water resources management and infrastructure planning (Danáčová et al., 2025).
Hydrograph patterns help assess the relationship between water level and flow rate using discharge rating curves, which are constructed from water level data across low to high flows (Soewarno, 1991). Therefore, it is also

Table 2. Suspended Load Classification

Suspended Load [ton ha^{-1} year^{-1}]	Class
SL ≤ 5	Very Low
5 < SL ≤ 10	Low
10 < SL ≤ 15	Medium
15 < SL ≤ 20	High
SL > 20	Very High

Source: Indonesian Minister of Environment Regulation No.61 Year 2014

necessary to analyze the structure of the hydrograph curve, which is divided into rising and falling phases, with the rising limb showing discharge increasing from baseflow to peak as water level expands the cross-sectional area and accelerates flow (Manuhana and Dibyosaputro, 2017). The rising phase is influenced by watershed characteristics such as flat slopes (0–8%), land cover, and rainfall intensity, where forests reduce discharge but regulate flow through runoff and infiltration (Sugianto et al., 2022). Rainfall intensity and duration also affect infiltration and surface flow, making this phase crucial for spatial planning and flood control, as reflected in the water level–discharge relationship.

Fig. 5 shows the relationship between water level and discharge in the rising phase, with R^2=0.90 indicating that 90% of the variation in discharge is explained by the regression model. This high coefficient of determination suggests that the power regression model is reliable for predicting discharge from water level data. In addition to the rising phase, the discharge rating curve was also developed for the falling (recession) phase of the hydrograph, which represents a gradual decrease in water level and discharge. The regression analysis for the falling phase produced an R^2 value of 0.98, indicating an even stronger model fit.

It is important to distinguish between R^2 and the correlation coefficient (r). While R^2 represents the proportion of variance in discharge explained by the model, r describes the strength and direction of the relationship between water level and discharge. In non-linear regression models, such as the power function used in this study, R^2 is not equal to r. Therefore, both parameters are reported separately to provide a more comprehensive evaluation of the relationship. Table 3 presents the discharge rating curve equations along with the corresponding r values for each hydrograph phase.

Table 3 shows r values of 0.95 (rising) and 0.99 (falling), indicating a very strong relationship between water level and discharge. This strong correlation suggests that the power regression model $Q = a \cdot (H)^b$ is appropriate for representing the relationship between the variables under the observed conditions. However, it should be noted that correlation reflects the strength of association and does not by itself determine model accuracy or measurement error. The high r values may also indicate relatively consistent hydrological responses during the observation period.

The correlation coefficient from the discharge curve was

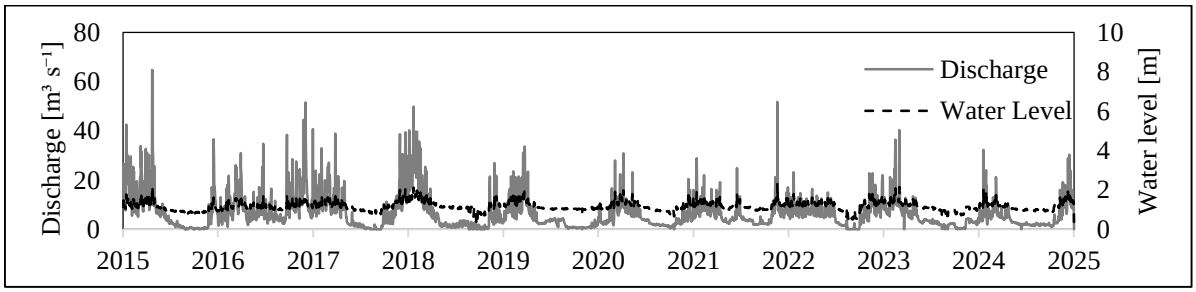


Fig. 4. Long-term hydrograph of the Bedog River displaying changes in discharge [m³ s⁻¹] and water level [m] from 2015 to 2024. The graph illustrates recurring seasonal fluctuations and several extreme flow events, showing the dynamic response of the watershed to hydrological condition.

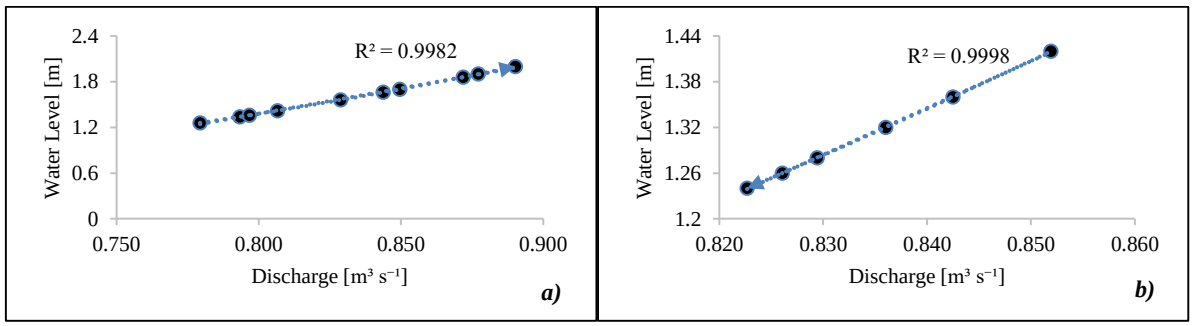


Fig. 5. Water level vs discharge in the rising (a) and falling (b) hydrograph.

Table 3. Results of discharge rating curve analysis

Analysis	Equation	Correlation (r)
Rising Hydrograph	$Q = 0.73 \cdot H^{0,29}$	0.95
Falling Hydrograph	$Q = 0.76 \cdot H^{0,26}$	0.99

compared with Manuhana (2017) in the Code watershed, showing r=0.991 (rising) and r=0.965 (falling). Both indicate a positive correlation consistent with this study, proving that Bedog River discharge increases with rising water level and decreases when it falls. The relationship between water level and discharge is influenced by the morphometry of the Bedog Sub-watershed, which covers 115.65 km². Larger watersheds can collect more rainwater, producing greater discharge, but respond more slowly to rainfall (Lee and Huang, 2016). The elongated shape of the watershed also affects flow, causing it to arrive gradually downstream. As a result, the increase in water level is slower and less extreme. This leads to smaller peak discharge and longer flood duration.

Correlation Between Discharge and Suspended Sediment Discharge

Stream discharge reflects watershed hydrology, while suspension discharge indicates sediment transport, with both closely linked as higher flow volume and velocity increase sediment movement, especially during floods or heavy rain. This relationship forms the basis of sediment transport models, often represented by the sediment rating curve (SRC), a power regression expressing their non-linear correlation. A single sediment curve cannot capture all flow conditions because rising and falling hydrograph phases differ: the rising phase increases discharge and kinetic energy, enhancing erosion and sediment transport, while in the falling phase sediment may remain high due to releases from the riverbed, demonstrating hysteresis (Efthimiou, 2019).

Fig. 6 shows the Q–Q_s relationship in the descending hydrograph, with an R^2 of 0.9895, meaning 98% of the variation is explained by the regression model. The falling phase results from changes in flow structure and sediment particles, with hysteresis affecting sediment load (Tabarestani and Zarrati, 2015). Although discharge remains high, reduced kinetic energy lowers transport capacity, causing particle deposition on the riverbed (Haddadchi and Hicks, 2021).

Sediment rating curve shows the relationship between flow discharge and the resulting sediment discharge. The sediment curve is used to estimate the relationship between the two data as an alternative to the limitations in data collection, namely not being able to observe detailed suspended sediment concentration data (Hapsari et al., 2019). Table 4 is the result of the sediment rating curve analysis that shows the value of the rising and falling hydrograph equations and their respective correlation values (r).

The correlation coefficients for the rising and falling hydrographs are 0.97 and 0.93, indicating a strong positive relationship between flow discharge and sediment discharge. This relationship is influenced by the Bedog Sub-watershed's morphometry: its elongated shape produces gradual flow and lower sediment discharge, while high drainage density accelerates rainwater into the river, increasing sediment transport potential. This pattern aligns with findings from the Batang Kuranji watershed (Utama et al., 2018).

Correlation with Spearman

To strengthen the results of the analysis, a Spearman's rank correlation test was conducted. The results of the correlation analysis obtained are presented as follows (Table 5).

The comparison between the two shows that the relationship between discharge and the observed parameters is slightly more consistent than that of sediment. This may be due to the fact that discharge is more directly influenced by hydrological factors, whereas sediment is more affected by river morphology, material types, and anthropogenic activities that increase data variability. Thus, the results confirm that both

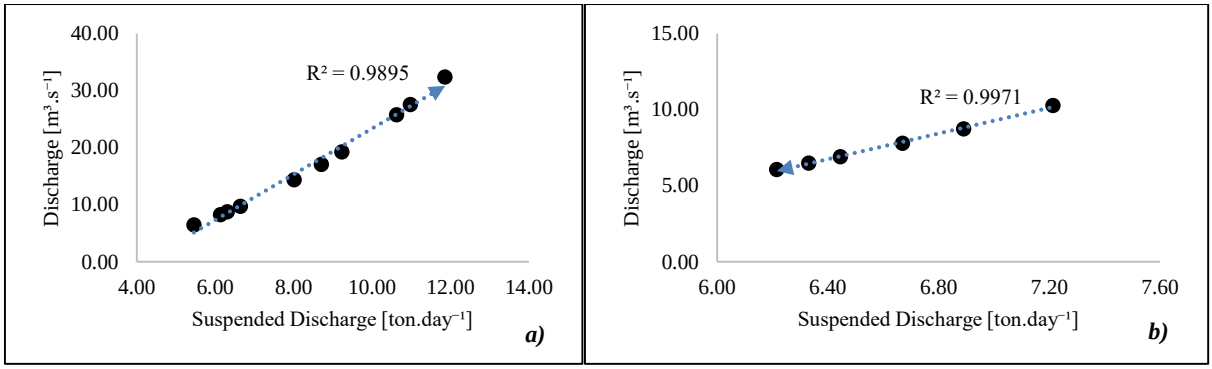


Fig. 6. Discharge vs suspended discharge in the rising (a) and falling (b) hydrograph.

Table 4. Results of sediment rating curve analysis

Analysis	Equation	Correlation (r)
Rising Hydrograph	$Q_s = 2{,}217 \cdot Q^{0{,}482}$	0.97
Falling Hydrograph	$Q_s = 3{,}730 \cdot Q^{0{,}283}$	0.93

discharge and sediment are closely related, with a higher stability observed in the discharge rating curve. These findings are consistent with Vercruysse et al. (2017), who demonstrated that uncertainties in sediment transport are generally greater than in discharge measurements.

Sediment Load Result

The sediment rating curve can estimate annual suspended sediment load by applying daily discharge data to the rising and falling hydrograph phases (Slabon and Hoffman, 2024). While calculations often use only the rising phase, which carries the highest sediment concentration (Manuhana and Dibyosaputro, 2017), this study considers both phases because each contributes to total suspended sediment. Sediment transport decreases in the falling phase as flow energy drops and more sediment deposits to the riverbed. Using both phases provides a more complete estimate of total load, with the rising phase capturing peak transport and the falling phase reflecting more stable flow conditions (Asselman, 1999). Daily discharge data that has been processed using the sediment arch equation is then summed to become data on the amount of suspended load in monthly and annual. The suspended load data obtained is in units of ton year^{-1}. The highest and lowest total suspended sediment loads of Bedog Sub-watershed according to the results of the 10-year calculation were 4550.29 ton in 2016 and 330.59 ton in 2019, detailed can be seen in Table 6.

The temporal distribution of these daily sediment loads over the study period is further visualized in Fig. 7. Based on this figure, there is a distinct annual seasonal pattern whereby sediment amounts increase significantly during the rainy season (October–April) and decrease during the dry season (April–October). However, the sediment loads are not constant throughout the year and are also influenced by extreme weather events that cause sporadic peaks in the data.

The data was then compared with research data from Manuhana and Dibyosaputro (2017) who calculated the results of a 10-year average of suspended sediment load on the Code River presented in monthly units with a total of 1,500.49 ton ha^{-1}. In general, the Bedog Sub-watershed suspended load is twice that of the Code River. This can be influenced by soil erosion and anthropogenic activities such as agriculture or land clearing that produce finer sediments and are easily carried as suspension. In addition, the Code River has a sabo dam that serves to retain volcanic sediment material from Mount Merapi. As a result, much of the sediment is retained in the sabo bag and does not reach the downstream (Manuhana and Dibyosaputro, 2017). In contrast, the Bedog Sub-watershed does not have such a large sediment control system, so sediment is more freely carried by the flow and increases its suspension load.

Fig. 8 shows the relationship between rainfall and suspended sediment load in the Bedog Sub-Watershed. A common pattern is that periods of high rainfall tend to be followed by an increase in the sediment load curve. The higher kinetic energy during periods of high rainfall can release more soil particles and result in significant surface runoff that transports sediment material to rivers. However, the relationship between rainfall and sediment load is not always linear. This can be seen in several months with maximum rainfall (e.g., throughout 2015–2018), where sediment load reached its highest peak (around 600 ton month^{-1} in 2018), but in other periods (e.g., 2024), relatively high rainfall did not always result in sediment loads as high as the previous peak. Although rainfall remains relatively stable and high throughout the year, sediment load fluctuates sharply, with peaks in 2016 and 2018 (500–600 ton month^{-1}) likely caused by extreme storms or increased sediment availability from severe erosion due to land-use changes. Conversely, low sediment levels (below 100 ton month^{-1}) indicate stable baseflow and low runoff, suggesting that land management and soil characteristics strongly influence erosion and sediment transport in the Bedog Sub-Watershed.

Fig. 9 presents the fluctuation of the average maximum discharge of Bedog Sub-watershed, Fig. 10 shows the fluctuation of the amount of suspension load of Bedog Sub-watershed from 2015 to 2024. Based on the two graphs, it can be seen that between the average maximum discharge and the amount of suspension in

Table 5. Results of Spearman Correlation Test

Test	Correlation
Discharge Rating Curve	0.998
Sediment Rating Curve	0.991

Table 6. Total suspended load in the Bedog Sub-Watershed from 2015 to 2024

Year	[ton year^{-1}]	Year	[ton year^{-1}]
2015	3914.19	2020	3689.42
2016	4550.29	2021	4052.96
2017	3838.99	2022	3807.24
2018	3623.71	2023	3557.35
2019	3360.59	2024	3737.20

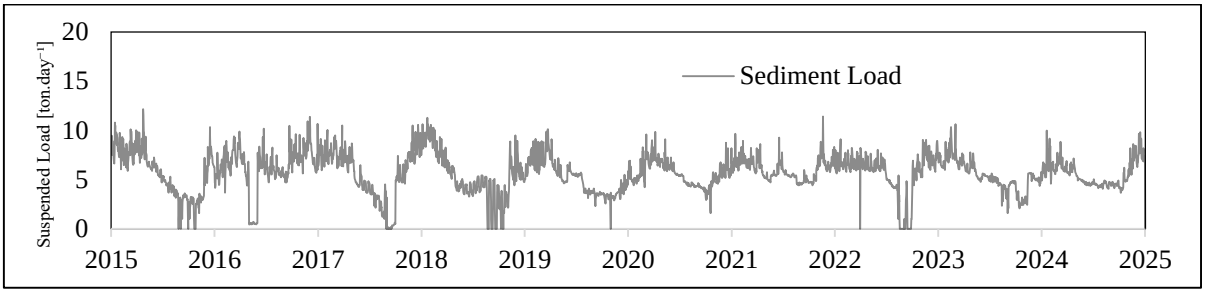


Fig. 7. Temporal variation of daily suspended sediment load in the Bedog-Sub watershed during 2015–2024.

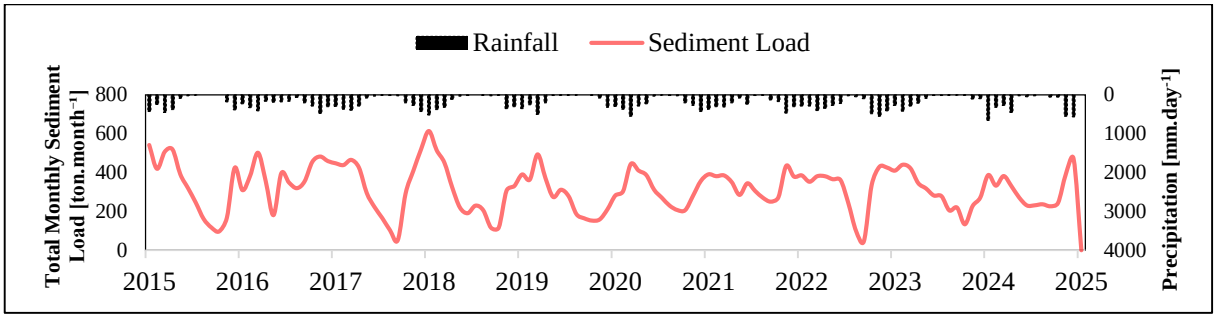


Fig. 8. Monthly total suspended sediment load [ton.month-1] and precipitation [mm.day-1] in the Bedog Sub-Watershed during 2015–2024. The red line represents sediment load variation, while the bars represent monthly rainfall.

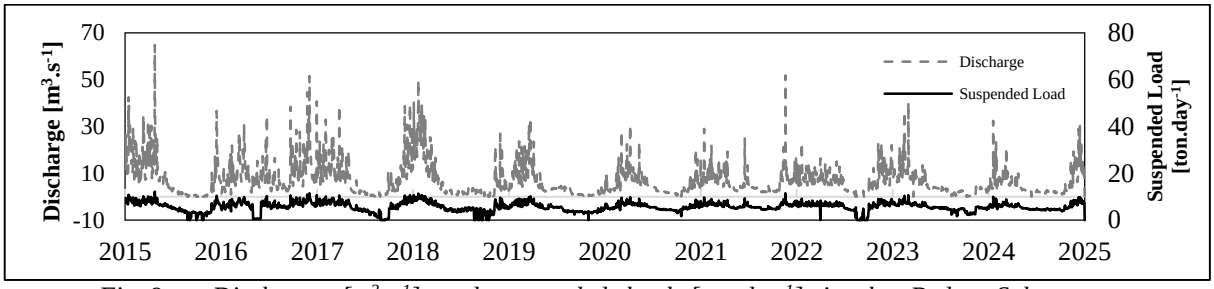


Fig. 9. Discharge [m3 s-1] and suspended load [ton day-1] in the Bedog Sub-Watershed during 2015–2024. The thin line represents discharge variation, while the bold line represent suspended load.

the Bedog Sub-watershed has the same trend pattern of increasing and decreasing. Both data decreased in 2016–2019 and 2019–2023. Meanwhile, the years 2015–2016, 2019–2021, and 2023–2024 experienced an upward trend.

Suspension data in ton ha^{-1} was divided by the Bedog Sub-watershed area (115.65 km²) to obtain sediment load per hectare. According to Indonesian Minister of Forestry Regulation No. 61/2014, sediment load is a key indicator for monitoring sub-watershed quality and continuity. It helps identify priority conservation areas for actions like reforestation, terracing, and small dam construction, as shown in Table 7 for 2015–2024.

From 2015–2024, sediment load in the Bedog Sub-watershed is classified as very low, with values ranging from 0.291 to 0.393 tons ha^{-1} year^{-1}. Sediment yield classification refers to Indonesian standards, where values of ≤ 5 ton ha^{-1} year^{-1} are categorized as very low, 5–10 ton ha^{-1} year^{-1} as low, 10–15 tons ha^{-1} year^{-1} as moderate, 15–20 ton ha^{-1} year^{-1} as high, and >20 tons ha^{-1} year^{-1} as very high. Based on this classification, the sediment yield in the study area falls within the very low category. It should be noted that the total sediment load presented in Table 6 (3360.59–4550.29 tons year^{-1}) represents annual values, whereas the classification is based on area-normalized sediment yield (tons ha^{-1} year^{-1} as shown in Table 7. The relatively low sediment yield is influenced by watershed characteristics, including its elongated shape, gentle slopes (0–8%), and site conditions. These features promote early sediment deposition, particularly in the mid-watershed, due to lower flow velocity and river morphology. Longer flow concentration times reduce peak discharge and flow kinetic energy, thereby limiting sediment transport capacity. As a result, sediment eroded from upstream areas is not fully transported downstream,

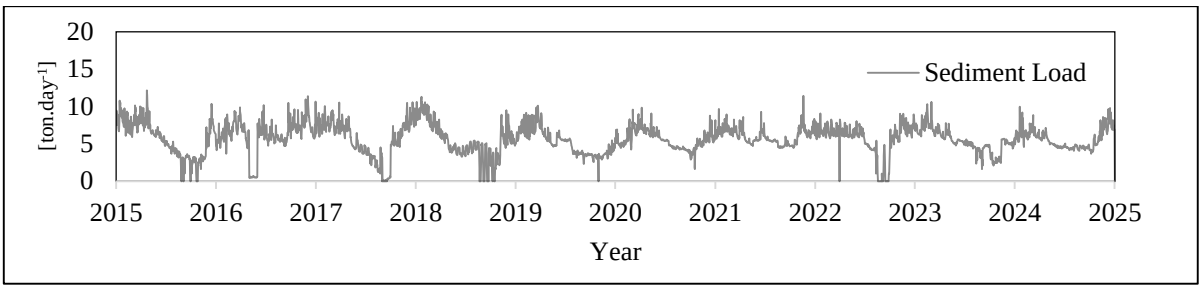


Fig. 10. Total Suspended Bedog Sub-Watershed in 2015–2024.

Table 7. Sediment Load Classification in the Bedog Sub-Watershed (2015–2024) per Indonesian Minister of Environment Regulation No. 61/2014

Year	[ton ha⁻¹ year⁻¹]	Classification	Year	[ton ha⁻¹ year⁻¹]	Classification
2015	0.338	Very Low	2020	0.319	Very Low
2016	0.393	Very Low	2021	0.350	Very Low
2017	0.332	Very Low	2022	0.329	Very Low
2018	0.313	Very Low	2023	0.308	Very Low
2019	0.291	Very Low	2024	0.323	Very Low

with deposition occurring along the flow path. In addition, sediment transport is influenced by land use, vegetation cover, and overall watershed geomorphology. The small sediment load is also influenced by total sediment, as this study only considers suspended sediment, not bedload. Sampling away from the watershed outlet can miss higher concentrations near the outlet, causing variability and potential bias in annual estimates (Thompson et al., 2020). Land conversion in the Bedog Sub-watershed, driven by expanding settlements, reduces vegetation cover (Prasena and Shresta, 2013). Less vegetation lowers soil infiltration, increasing surface runoff, which in turn accelerates erosion and sedimentation. Compared to Yustika et al. (2019), sediment load in the Bedog Sub-watershed is 31 times lower than Sekampung Hulu (141.3 km²) and 14 times lower than Sangharus (117.2 km²). Estimated suspended sediment is generally lower than observed values (Boukhrissa et al., 2013). Despite being very low, management and monitoring remain essential to sustain the Bedog Sub-watershed.

Conclusion

In the Bedog Sub-watershed, water level and stream discharge exhibit a strong positive correlation (0.95–0.99), between water level elevations and discharge. The watershed's small area and elongated shape result in rapid but gradual flows, lower peak discharge, and longer flood duration. River discharge and suspended sediment also show a strong positive relationship (r=0.97 rising, 0.93 falling), as higher flows carry more sediment, influenced by watershed morphometry and high drainage density. Estimated suspended sediment in the downstream area from 2015–2024 ranges from 3,360.59 to 4,550.29 tons year⁻¹, yet sediment load per hectare remains very low (0.291–0.393 tons ha⁻¹ year⁻¹ affected by watershed size, shape, slope, sediment control structures, and sampling location limitations.

Acknowledgement

The author would like to express sincere gratitude to all parties who have supported the completion of this research, especially Universitas Gadjah Mada which support this research under the Final Assignment Recognition (Rekognisi Tugas Akhir) project number 4193/UN1.P1/Dit-Lit/PT.01.03/2025. Special thanks are extended to Department of Environment and Forestry of Yogyakarta Province provided data for the research. This study would not have been possible without the contributions and encouragement from everyone involved.

References

Adhitama, S. Y., Musthofa, A., Rohmah, A. A., Nurwidiani, T., Sejati, M. A., Wati, E. T., Saputro, R., Rachmawati, R., Nurjani, E., Sudrajat (2022): The strategies of sustainable watershed management at bedog sub-watershed, special region of yogyakarta. *IOP Conference Series: Earth and Environmental Science, 1039*(1), 1–11.

American Public Health Association (APHA), AWWA, WEF. (2017): *Standard Methods for the Examination of Water and Wastewater* (23rd ed.). Washington, DC: APHA.

Asselman, N. E. (1999): *Suspended Sediment in the River Rhine: Suspended Sediment Concentrations During High Discharge Events*. Utrecht: Faculty of Spatial Sciences Utrecht University.

Asrul, A., Eraku, S., Agu, R. R., Maini, A. A., Lasamu, M., Massi, S. (2025): Pengaruh alih fungsi lahan terhadap kejadian banjir di Kelurahan Leato Selatan Kecamatan Kota Timur Kota Gorontalo. *Geodika: Jurnal Kajian Ilmu dan Pendidikan Geografi, 9*(1), 52–61.

Astuti, F. A., Lukito, H. (2020): Perubahan penggunaan lahan di kawasan keamanan dan ketahanan pangan di Kabupaten Sleman. *Jurnal Geografi: Media Informasi Pengembangan dan Profesi Kegeografian*, *17*(1), 1–6.

Bonacci, O., Žaknić-ćatović, A., Roje-Bonacci, T. (2025): Detecting subtle hydrological changes in a small basin in a changing climate: The Bednja River case. *Acta Hydrologica Slovaca*, *26*(2), 306–317. https://doi.org/10.31577/ahs-2025-0026.02.0031

Boukhrissa, Z. A., Khanchoul, K., Le Bissonnais, Y., Tourki, M. (2013): Prediction of sediment load by sediment rating curve and neural network (ann) in El Kebir Catchment, Algeria. *Journal of Earth System Science*, *122*, 1303–1312.

Danáčová, M., Jeihouni, E., Bacigál, T., Výleta, R., Danáčová, Z., Szolgay, J. (2025): Travel-time–discharge modelling for flood routing with broken line regression on the Morava River. *Acta Hydrologica Slovaca*, *26*(2), 337–346. https://doi.org/10.31577/ahs-2025-0026.02.0034

Dorneles, V. R., Wojahn, V.S., Beskow, S., Nunes, M. C. M. (2024): Applicability of sediment rating curves: analysis in the state of rio grande do sul. Revista Brasileira de Geografia Física, 17(4):3037–3051.

Efthimiou, N. (2019): The role of sediment rating curve development methodology on river load modelling. *Environmental Monitoring Assess*, *191*, 108.

Haddadchi, A., Hicks, M. (2021): Interpreting event-based suspended sediment concentration and flow hysteresis patterns. *Journal of Soils and Sediments*, *21*, 592–612.

Hapsari, D., Onishi, T., Imaizumi, F., Noda, K., Senge, M. (2019): The use of sediment rating curve under its limitations to estimate the suspended load. *Reviews in Agricultural Science*, *7*, 88–101.

Hermawan, S. G., Suprayogi, S., Fadlillah, L. N. (2025): Soil and water assessment tool (swat) model for hydrological response analysis in the Gajahwong Subwatershed, Yogyakarta, Indonesia. *Journal of Degraded and Mining Lands Management*, *12*(2), 7287–7299.

Hicks, D. M., Fenwick, J. K. (1994): Suspended sediment manual. New Zealand: NIWA.

Lee, K. T., Huang, J. K. (2016): Influence of storm magnitude and watershed size on runoff nonlinearity. *Journal of Earth System Science*, *125*(4), 777–794.

Mahmood, A., Han, J. C., Ijaz, M. W., Siyal, A. A., Ahmad, M., Yousaf, M. (2022): Impact of sediment deposition on flood carrying capacity of an alluvial channel: a case study of the Lower Indus Basin. *Water*, *14*(20), 3321.

Manuhana, R. J., Dibyosaputro, S. (2017): Kajian muatan sedimen tersuspensi di Sungai Code Daerah Istimewa Yogyakarta. *Jurnal Bumi Indonesia*, *6*(4).

Mukaka, M. M. (2012): *A guide to appropriate use of correlation coefficient in medical research*. Malawi Medical Journal, 24(3), 69–71.

Nuraida, Yamani, S. A. Z., Azhar, R., Safitri, A., Fahri, Z. (2024): Analisis erosi tanah akibat alih fungsi lahan hutan di Sub-DAS Krueng Meuh Aceh. *Jurnal Galung Tropika*, *13*(3), 357–368.

Peraturan Menteri Kehutanan Republik Indonesia Nomor 61 Tahun 2014. (2014): *Peraturan menteri kehutanan republik indonesia nomor 61 tahun 2014 tentang monitoring dan evaluasi pengelolaan daerah aliran sungai*. Jakarta: Pemerintah Pusat Indonesia.

Prasena, A., Shrestha, D. B. (2013): Assessing the effects of land use change on runoff in Bedog Sub Watershed Yogyakarta. *Indonesian Journal of Geography*, *45*(1), 48–61.

Rantz, S. E., et al. (1982): *Measurement and Computation of Streamflow: Volume 2. Computation of Discharge*. U.S. Geological Survey Water-Supply Paper 2175.

Setiawan, F., Basuki, T. M., Santosa, B. H., Pramono, I. B., Chulafak, G. A., Rahmadya, A., Nada, F. M. H. (2025): Developing algorithms for estimating total suspended solids (tss) using unmanned aerial vehicle: a case study in the upper Citarum River, Indonesia. *Journal of Degraded Mining Lands Management*, *12*(2), 7379–7388.

Shenliang, C., Guoan, Z., Shilun, Y. (2003): Temporal and spatial changes of suspended sediment concentration and resuspension in the Yangtze River Estuary. *Journal of Geographical Sciences*, *13*(4), 498–506.

Slabon, A., Hoffman, T. (2024): Uncertainties of annual suspended sediment transport estimates driven by temporal variability. *Water Resources Reseacrh*, *60(*1).

Soewarno (1991): *Hidrologi Pengukuran dan Pengolahan Data Aliran Sungai Hidrometri*. Bandung: Penerbit Nova.

Sugianto, S., Deli, A., Miswar, E., Rusdi, M., Irham, M. (2022): The effect of land use and land cover changes on flood occurrence in Teunom Watershed, Aceh Jaya. *Land*, *11*(8), 1271.

Suprayogi, S., Gunawan, T., Murti, S. H., Endarto, R., Prihartanto, W. J., Widodo, N. A. (2019). Kondisi hidrologi terkait dengan perubahan penggunaan lahan DAS Bedog Kabupaten Sleman. *Majalah Geografi Indonesia*, *33*(2), 29–36.

Tabarestani, M. K., Zarrati, A. R. (2015): Sediment transport during flood event: a review. *International Journal of Environmental Science and Technology*, *12*, 775–788.

Thompson, J., Pelc, C. E., Jordan, T. E. (2020). Water quality sampling methods may bias evaluations of watershed management practices. *Science of the Total Environment, 765*, 142739.

Utama, L., Saidi, A., Berd, I., Mizwar, Z. (2018): Kajian morphometri pada daerah aliran sungai (DAS) Batang Kuranji Terhadap Debit Banjir. *FRONTIERS: Jurnal Sains dan Teknologi*, *1*(1), 65–79.

Vercruysse, K., Grabowski, R. C., Rickson, R. J. (2017): Suspended sediment transport dynamics in rivers: multi-scale drivers of temporal variation. *Earth-Science Reviews*, 166, 38–52.

Walpole, R. E., Myers, R. H., Myers, S. L., Ye, K. (2012): *Probability and Statistics for Engineers and Scientists* (9th ed.). Pearson Education.

Yustika, R, D., Somura, H., Yuwono, S. B., Arifin, B., Ismono, H., Masunaga, T. (2019):_ Assessment of soil erosion in social forest-dominated Watersheds in Lampung, Indonesia. *Environmental Monitoring Assessment. 191* (726).

Aqila Rheva Latifah Ibrahim
Dr. Lintang Nur Fadlillah (*corresponding author, e-mail: lintang.n.f@ugm.ac.id)
Department of Environmental Geography
Faculty of Geography, Universitas Gadjah Mada
Yogyakarta 55281
Indonesia